ISBN: 978-3-95450-216-5 doi:10.18429/JACoW-eeFACT2018-MOYAA01

SEVERAL TOPICS ON BEAM DYNAMICS IN FCC-ee*

K. Oide†, KEK, Tsukuba, Japan
D. Shatilov, BINP SB RAS, Novosibirsk, Russia
S. Aumon, T. K. Charles, D. El Khechen, T. Tydecks, CERN, Geneva, Switzerland

Abstract

The FCC-ee is a double-ring e^+e^- collider to be installed in a common tunnel of ~ 100 km circumference, as a potential first step before the FCC-hh hadron collider. Several studies on the beam dynamics at FCC-ee: low emittance tuning, dynamic aperture, beam blowup with/without beam beam, are introduced in the paper.

INTRODUCTION

The beam energy of FCC-ee covers at least from the Z-pole (45.6 GeV) to $t\bar{t}$ (182.5 GeV). The design luminosity is the highest ever at each energy, under the constraint that the synchrotron radiation (SR) power is less than 100 MW for the total of two beams. The design is based on existing technologies verified in e^+e^- colliders in the world, including VEPP-IV, LEP, PEP-II, KEKB, DAΦNE, BEPC II, SuperKEKB. The main characteristics of the optics design [1] have been double ring, with ~ 100 km circumference, two interaction points (IPs) per ring, horizontal crossing angle of 30 mrad at the IP, and the crab-waist scheme with local chromaticity correction system. A so-called "tapering" of the magnets is applied, which scales all fields of magnets with the local beam energy determined by the SR. An asymmetric layout near the interaction region suppresses the critical energy of SR incoming to the detector at the IP below 100 keV. Sufficient transverse/longitudinal dynamic apertures (DAs) have been obtained to assure adequate beam lifetime with beamstrahlung and top-up injection. Table 1 lists the basic parameters of FCC-ee. For the estimation of the running plan at each energy, luminosities less than numbers in this table by 10–20% are used at each energy to have a margin for operation.

LOW EMITTANCE TUNING WITH DYNAMIC APERTURE

Due to the low emittance budget and the small β^* at the interaction point, the FCC-ee is a challenging accelerator to correct when misalignments are introduced in the simulations. These errors produce a large vertical dispersion (several hundred meters without any correction applied) and coupling, which compromise the target emittances, in particular at high energy. Several correction methods and algorithms were developed in order to preserve the emittances as close as possible to their design values.

Horizontal correctors were installed at every focusing quadrupole and vertical correctors at every defocusing quadrupole. Beam Position Monitors (BPM) were placed at each quadrupole, including at the doublet of the IPs. Skew quadrupole correctors with a trim quadrupole are placed at the sextupoles to correct the beta-beat and rematch the horizontal dispersion. Special skew quadrupoles were installed in the interaction region to compensate the tilt of the doublet quadrupoles at the IPs. The effect of the tilt of dipoles and field errors will be included in the next phase of the study. The vertical dispersion distortion was corrected with orbit correctors via the dispersion free steering method [2] first and with skew quadrupoles with the help of response matrices. The linear coupling was corrected by adjusting the linear coupling resonance driving term parameters, as tested at the ESRF [3]. Trim quadrupoles were used to rematch the phase advances between the BPMs, again using response matrices. Satisfactory results for the misalignment tolerance were found when the magnets were misaligned as defined in Table 2.

1000 seeds were tested with the correction algorithm using the input misalignments listed in Table 2 and 70% of them converged, as shown in Fig. 1, with the following results for the emittances:

$$\epsilon_y = 0.10 \pm 0.013 \text{ pm}$$
$$\epsilon_x = 1.52 \pm 0.01 \text{ nm}$$
$$\epsilon_y/\epsilon_x = 0.0065\%$$

More studies are going on with less number of orbit correctors using trim windings on the arc sextupoles, with more machine errors including the roll of dipoles, misalignments taking the scheme of girders into account, and BPM errors [4].

The resulting dynamic aperture (DA) at $t\bar{t}$ has been evaluated as shown in Fig. 2. The average of them are just on the design DA. The variation is within the margin for the plan of the integrated luminosity.

DYNAMIC AND MOMENTUM APERTURE OPTIMIZATION USING PSO

Applying particle swarm optimization (PSO) in accelerator physics to improve machine parameters is a worthwhile method to cope with the increasingly large number of degrees of freedom to optimize. With an existing machine it is possible to optimize the sextupole setting by improving dynamic aperture through lifetime optimization using PSO [5].

* Work supported by the European Commission under Capacities 7th Framework Programme project EuCARD–2, grant agreement 312453, and under the Horizon 2020 Programme project CREMLIN, grant agreement 654166.
† katsunobu.oide@cern.ch

ISBN: 978-3-95450-216-5 doi:10.18429/JACoW-eeFACT2018-MOYAA01

Table 1: Machine parameters of the FCC-ee for different beam energies

		Z	WW	ZH	tt̄	
Circumference	[km]			97.756		
Bending radius	[km]			10.760		
Free length to IP ℓ^*	[m]			2.2		
Solenoid field at IP	[T]			2.0		
Full crossing angle at IP	[mrad]			30		
SR power / beam	[MW]			50		
Beam energy	[GeV]	45.6	80	120	175	182.5
Beam current	[mA]	1390	147	29	6.4	5.4
Bunches / beam		16640	2000	328	59	48
Average bunch spacing	[ns]	19.6	163	994	2763[a]	3396[a]
Bunch population	[10^{11}]	1.7	1.5	1.8	2.2	2.3
Horizontal emittance ε_x	[nm]	0.27	0.84	0.63	1.34	1.46
Vertical emittance ε_y	[pm]	1.0	1.7	1.3	2.7	2.9
Arc cell phase advances	[deg]	60/60		90/90		
Momentum compaction α_p	[10^{-6}]	14.8		7.3		
Arc sextupole families		208		292		
Horizontal β_x^*	[m]	0.15	0.2	0.3	1.0	
Vertical β_y^*	[mm]	0.8	1.0	1.0	1.6	
Horizontal size at IP σ_x^*	[µm]	6.4	13.0	13.7	36.7	38.2
Vertical size at IP σ_y^*	[nm]	28	41	36	66	68
Energy spread (SR/BS) σ_δ	[%]	0.038/0.132	0.066/0.131	0.099/0.165	0.144/0.186	0.150/0.192
Bunch length (SR/BS) σ_z	[mm]	3.5/12.1	3.0/6.0	3.15/5.3	2.01/2.62	1.97/2.54
Piwinski angle (SR/BS)		8.2/28.5	3.5/7.0	3.4/5.8	0.8/1.1	0.8/1.0
Length of interaction area L_i	[mm]	0.42	0.85	0.90	1.8	1.8
Hourglass factor R_{HG}						
Crab sextupole strength	[%]	97	87	80	40	40
Energy loss / turn	[GeV]	0.036	0.34	1.72	7.8	9.2
RF frequency	[MHz]	400			400 / 800	
RF voltage	[GV]	0.1	0.75	2.0	4.0 / 5.4	4.0 / 6.9
Synchrotron tune Q_s		0.0250	0.0506	0.0358	0.0818	0.0872
Long. damping time	[turns]	1273	236	70.3	23.1	20.4
RF acceptance	[%]	1.9	3.5	2.3	3.36	3.36
Energy acceptance (DA)	[%]	±1.3	±1.3	±1.7	-2.8 +2.4	
Polarisation time t_p	[min]	15000	900	120	18.0	14.6
Luminosity / IP	[10^{34}/cm^{2}s]	230	28	8.5	1.8	1.55
Horizontal tune Q_x		269.139	269.124	389.129	389.108	
Vertical tune Q_y		269.219	269.199	389.199	389.175	
Beam-beam ξ_x/ξ_y		0.004/0.133	0.010/0.113	0.016/0.118	0.097/0.128	0.099/0.126
Allowable e^+e^- charge asymmetry	[%]	±5	±3			
Lifetime by rad. Bhabha	[min]	68	59	38	40	39
Actual lifetime by BS	[min]	> 200	> 200	18	24	18

[a] A half ring is filled with the common rf scheme

Table 2: Tolerances for misalignments and roll for arc quadrupoles, sextupoles, and the IP quadrupoles." This could be changed to "Misalignment errors introduced to the lattice before correction applied. Misalignments and roll angles applied randomly with a probability governed by a Gaussian distribution (truncated at 2.5 σ) with the a standard derivation values as stated.

Magnet type	σ_x µm	σ_y µm	θ µrad
Arc quadrupoles	100	100	100
Sextupoles	100	100	0
IP quadrupoles	50	50	50

A particle swarm optimizer is a kind of genetic algorithm with both cognitive and social components, originally influenced by bird flocking behavior [6]. PSO can be employed to improve dynamic and momentum aperture of FCC with its high number of degrees of freedom.

In the case of FCC-ee, the number of degrees of freedom may be reduced by keeping the proposed $-\boldsymbol{I}$ transform between sextupole pairs, and additionally maintaining periodicity of the machine after each half-turn. Doing so, there are 294 degrees of freedom left. This number is clearly out of range for brute force scanning and genetic algorithms like PSO are better equipped to handle the optimization.

The optimizer improves the objective function(s) over time by iteratively adjusting position and speed of the candidate solutions (particles) in search space:

$$\vec{x}_{n+1} = \vec{x}_n + \vec{v}_{n+1}, \quad (1)$$

$$\vec{v}_{n+1} = \omega\vec{v}_n + c_c r_1(\vec{x}_{\text{p-best}} - \vec{x}_n) + c_s r_2(\vec{x}_{\text{g-best}} - \vec{x}_n)\,. \quad (2)$$

Here, $\vec{x}$ is the position in search space, which in this scenario would be a vector containing the individual sextupole strengths, $\vec{v}$ is the velocity (change of position per generation) of the individual particle in search space. Additionally,

ISBN: 978-3-95450-216-5 doi:10.18429/JACoW-eeFACT2018-MOYAA01

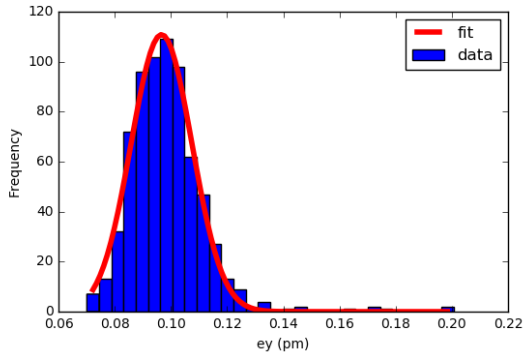

Figure 1: Statistical distribution of the vertical emittance for 700 different seeds resulting from the input misalignments given in Table 2. Initially 1000 seeds were tested and 70% of them converged.

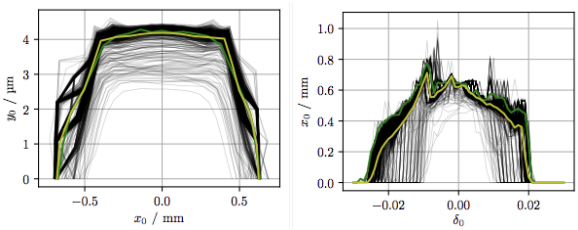

Figure 2: Variation of the dynamic aperture with the misalignment after correction for converged samples, transverse (left) and momentum (right).Evaluated at $t\bar{t}$ with tapering by MADX/PTC.

there is $\vec{x}_{\text{p-best}}$, which is the position where the individual particle has best performed in its history, and $\vec{x}_{\text{g-best}}$, which is the global best position known so far. The velocity for the next generation $\vec{v}_{n+1}$ therefore depends on

- the initial velocity $\vec{v}_n$, weighted by factor ω, describing the rigidity of movement,
- the individual particles personal best solution $\vec{x}_{\text{p-best}}$, weighted by cognitive factor c_c,
- the global best solution $\vec{x}_{\text{g-best}}$, weighted by social factor c_s.

Based on tracking dynamic and momentum aperture for different candidate solutions, candidates are assigned a score (value function in Fig. 3) which makes them more or less successful in their impact on the population. With the way the value function is set, the algorithm may be steered towards favoring one objective over another (e. g. favoring area of momentum aperture over area of dynamic aperture).

The particles are initialized with the sum of a vector containing the reference sextupole setting and a random vector, with maximum change in k_2 per sextupole of 0.01 m^{-2}.

The solution presented here is found in the 17$^{\text{th}}$ generation. It yields an improvement of the area of momentum aperture of 18.0 % compared to the reference lattice, as shown in Fig. 4.

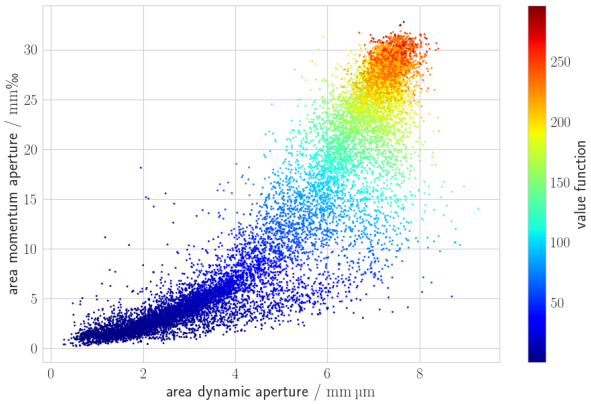

Figure 3: Value function as a function of area of momentum aperture and area of dynamic aperture for all solutions of the PSO algorithm.

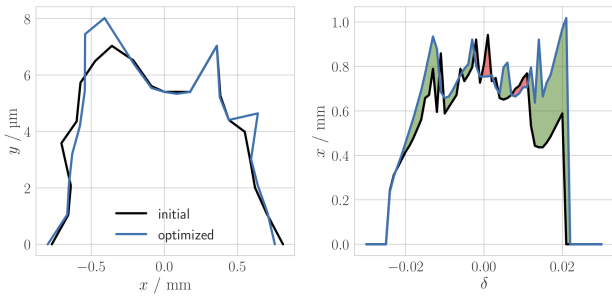

Figure 4: Dynamic aperture (left) and momentum aperture (right) for reference lattice (black) and optimized lattice (blue). The area of dynamic aperture is improved by 3.1 % while the area of momentum aperture is increased by 18.0 %.

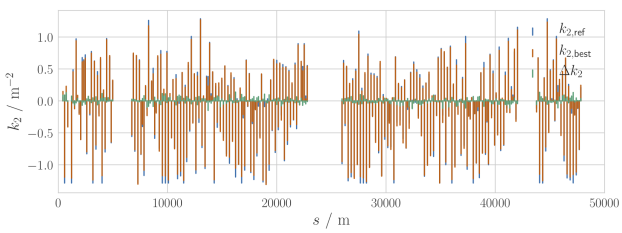

Figure 5: Change in sextupole strengths (green) between optimized solution (red) and reference solution (blue) for one half ring.

In Fig. 5, the change of k_2 between the optimized solution and the reference solution is presented. Although at first glance the solution appears to be as arbitrary as the reference setting, when looking closely at the peak sextupole strengths a difference can be observed: the peak sextupole strengths appear to have been reduced by the optimizer compared to the reference setting.

ISBN: 978-3-95450-216-5 doi:10.18429/JACoW-eeFACT2018-MOYAA01

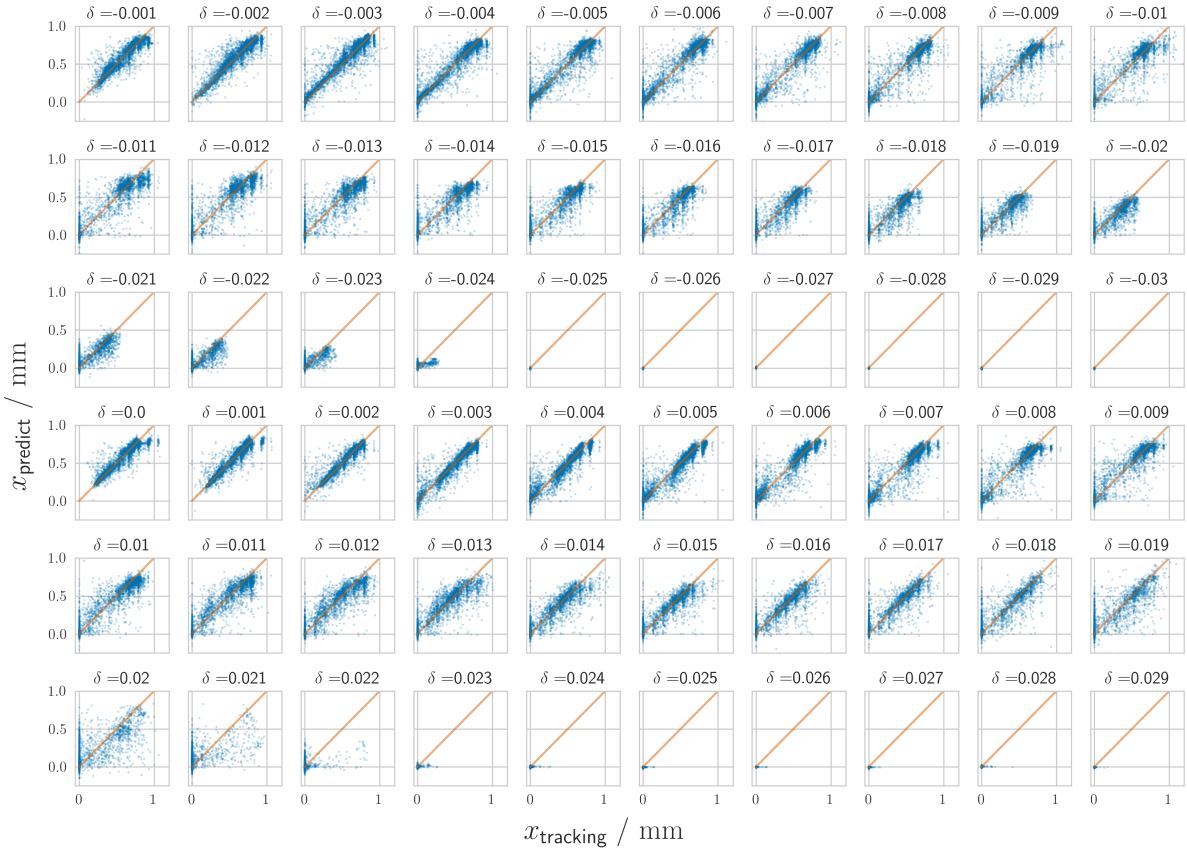

Figure 6: Aperture predictions for different energy deviations of trained model together with true values from particle tracking determined for a test data set (which has been withheld from training).

Prospects of Employing Machine Learning Concepts for PSO

As a side effect of the optimization, a large number of sextupole settings has been investigated regarding dynamic / momentum aperture (comp. Fig. 3). These settings can be used to train an artificial neural network (NN) to predict resulting momentum aperture for different sextupole settings. With this model, the optimization process can be significantly accelerated since time consuming particle tracking can be avoided.

As a proof of principle, a NN containing an input layer, three hidden layers, and an output layer has been tested. As input, the NN takes the 298 sextupole strengths (including final focus). The hidden layers all accept 300 input values and produce 300 output values. The output layer is the 61 horizontal apertures for different energy deviations ranging from −3 % to 3 % in steps of 1 ‰. First results indicate reasonably good agreement with the predictions by the trained model and the actual data for a test data set, withheld from training (comp. Fig. 6).

However, for large energy deviations, the trained model fails to reproduce tracked apertures. Since the training data set contains only small apertures for large energy deviations, the model will assume that any combination of sextupole strengths must lead to small apertures for large energy deviations.

Nevertheless, the trained model itself can be used in a PSO algorithm, performing the formerly time consuming step of determining the aperture in a matter of milliseconds. Doing so, the model can be used to enhance aperture for energy deviations in a range where the training data set found considerable aperture already. By testing promising candidates through tracking, the training data set (and the model) may be continuously enhanced with respect to large energy deviation apertures.

Thus, a shortcut in optimizing dynamic aperture can be provided. Furthermore, it is possible to evaluate different objective functions, e. g. favoring particular shapes of aperture, based on the trained model. In addition, analysis of the trained model might provide insight into which sextupoles have less impact on dynamic aperture compared to others, in order to mainly use those for chromaticity correction.

In a future application, machine learning can be used to optimize the repopulating step in PSO. By intervening in the evolution process through selecting high potential candidates whilst maintaining diversity, the optimization process can be significantly enhanced as has been shown in the light source community [7].

ISBN: 978-3-95450-216-5 doi:10.18429/JACoW-eeFACT2018-MOYAA01

UNEXPECTED BEAM BLOWUP

A blowup of vertical emittance has been observed in particle tracking simulations with beam-beam and lattice misalignments [8]. Its was somewhat unexpected, since estimation without lattice errors did not predict such a blowup unless a residual vertical dispersion at the interaction point (IP) is larger than a certain amount. Table 3 shows the such a criteria on the residual dispersion at the IP. The beam-beam simulations were done by SAD [9] with BBWS weak-strong model implemented within it [10]. Even beam-beam simulations with lattice without misalignments did not show such blowup [11].

Table 3: Tolerances for residual dispersions at the IP for each energy of FCC-ee, obtained by quasi strong-weak model without lattice. The tolerance $\Delta\eta_y^*$ corresponds to 5% increase of vertical beam size σ_y^* at the IP with beamstrahlung.

Beam energy [GeV]	45.6	80	120	175
Design σ_y^* [nm]	28	41	35	66
Energy spread[a] [%]	0.13	0.13	0.165	0.185
$\Delta\eta_y^*$ [μm]	1	5	4	6

[a] with beamstrahlung

Figure 7 shown an example of such a blowup for two seeds of random numbers of misalignments of arc sextupoles. Note that the residual dispersion at the IP for seed 3 is smaller than the previous criteria given in Table 3, while giving even larger blowup than another seed 19, which has larger dispersions at the IP.

Later it was found that such a blowup happens only by lattice coupling/dispersion without beam-beam. Then it was shown that this is a effect called "anomalous emittance" as described in Ref. [12], caused by synchro-beta resonance with the lattice chromaticity in the x-y coupling and dispersion. Such a phenomenon can be described by a Vlasov model in the synchrotron phase space. See a detailed description in Ref. [13]. This kind of blowup is intrinsic to a lattice with chromatic dispersions and x-y coupling. Mitigations are possible by a low emittance tuning toward well below the design emittance ratio combined with a better choice of operating tunes.

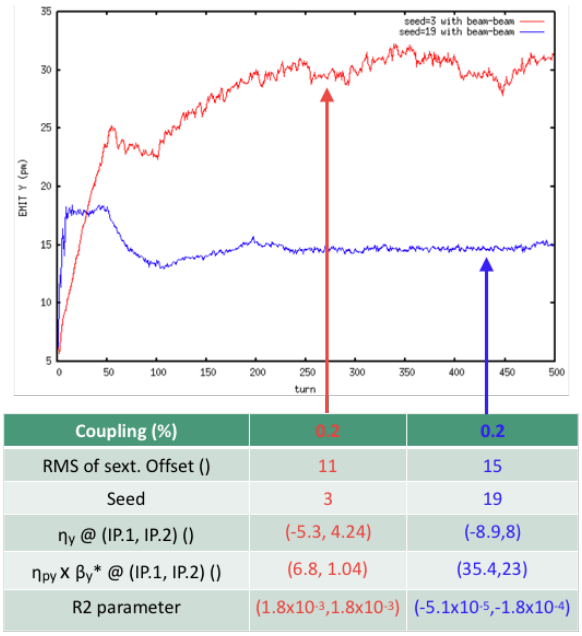

Coupling (%)	0.2	0.2
RMS of sext. Offset ()	11	15
Seed	3	19
η_y @ (IP.1, IP.2) ()	(-5.3, 4.24)	(-8.9,8)
η_{py} x β_y* @ (IP.1, IP.2) ()	(6.8, 1.04)	(35.4,23)
R2 parameter	(1.8×10^{-3},1.8×10^{-3})	(-5.1×10^{-5},-1.8×10^{-4})

Figure 7: Blowup of vertical emittance measured at he IP by a particle tracking with beam-beam, beamstrahlung, and lattice. The arc sextupoles are vertically misaligned randomly to produce the vertical emittance of the design ratio $\varepsilon_y/\varepsilon_x = 0.2\%$. Two examples for different seeds are shown, corresponding residual vertical dispersions at the IP in the table.

ACKNOWLEDGEMENT

The authors thank M. Benedikt, A. Blondel, M. Boscolo, E. Levichev, K. Ohmi, D. Zhou, F. Zimmermann, and the entire FCC-ee Collaboration Tefor encouraging the research, useful discussions, and suggestions.

REFERENCES

[1] K. Oide, *et al.*, *Phys. Rev. Accel. Beams* 19 (2016) no.11, 111005.
[2] R. Assmann, P. Raimondi, G. Roy and J. Wenninger, "Emittance optimization with dispersion free steering at LEP", *Phys. Rev. ST Accel. Beam*, **3**,p. 121001(2000).
[3] A. Franchi *et al*, "Vertical emittance reduction and preservation in electron storage rings via resonance driving terms correction", *Phys. Rev. ST Accel. Beam*, **14**, p. 034002(2015).
[4] T. K. Charles, presented at eeFACT2018, Hong Kong, Sep 2018, paper TUOAB02, this conference.
[5] Li, Yongjun and Cheng, Weixing and Yu, Li Hua and Rainer, Robert, "Genetic algorithm enhanced by machine learning in dynamic aperture optimization", *PRAB* **21**,p.054601(2018).
[6] R. Eberhart and J. Kennedy, "A new optimizer using particle swarm theory", *MHS'95. Proc of the Sixth International Symposium on Micro Machine and Human Science*, pp.39–43(1995).
[7] Li, Yongjun and Cheng, Weixing and Yu, Li Hua and Rainer, Robert, "Genetic algorithm enhanced by machine learning in dynamic aperture optimization", *Phys. Rev. Accel. Beams*, **21**, 5, p. 11 (2018).
[8] D. El Khechen, presented at eeFACT2018, Hong Kong, Sep 2018, paper TUYBA03, in this conference.
[9] `http://acc-physics.kek.jp/SAD/index.html`, `https://github.com/KatsOide/SAD`
[10] K. Ohmi, *et al.*, "BEAM-BEAM SIMULATION STUDY FOR CEPC", THPRI003, *IPAC'14* (2014).
[11] D. Zhou, presented at FCC Week 2016, 11–15 April 2016, Rome, Italy(2016).
[12] K. Oide and H. Koiso, "Anomalous equilibrium emittance due to chromaticity in electron storage rings", *Phys.Rev. E49* pp. 4474-4479(1994).
[13] K. Oide, presented at eeFACT2018, Hong Kong, Sep 2018, paper WEXBA03, in this conference.